Available online at www.sciencedirect.com
ScienceDirect
Journal of Sound and Vibration 322 (2009) 216–226
JOURNAL OF SOUND AND VIBRATION
www.elsevier.com/locate/jsvi

In-plane free vibration of circular annular disks

S. Bashmal*, R. Bhat, S. Rakheja

Department of Mechanical and Industrial Engineering, Concordia University, 1455 De Maisonneuve Boulevard West, Montreal, Quebec, Canada H3G 1M8

Received 28 February 2008; received in revised form 26 August 2008; accepted 7 November 2008
Handling Editor: S. Bolton
Available online 23 January 2009

Abstract

This paper presents a generalized formulation for the in-plane modal characteristics of circular annular disks under combinations of all possible classical boundary conditions. The in-plane free vibration of an elastic and isotropic disk is studied on the basis of the two-dimensional linear plane stress theory of elasticity. The boundary characteristic orthogonal polynomials are employed in the Rayleigh–Ritz method to obtain the natural frequencies and associated mode shapes. Two approaches have been used to represent a clamped boundary condition. The first approach assumes a polynomial expression that satisfies the clamped conditions, while the second approach uses a disk with free boundary supported on artificial springs with stiffness tending to infinity. The natural frequencies are tabulated and compared with data available in the literature. Mode shapes are presented to illustrate the free vibration behavior of the disk.

1. Introduction

Circular disks are commonly used in a wide variety of engineering applications including space structures, electronic components and rotating machinery. While there is a vast amount of information available on the out-of-plane vibration of plates, the studies reported on the in-plane vibrations of circular annular disks is relatively scarce [1–4]. Although some studies included in-plane dynamics in the analysis, the focus was towards the instabilities of out-of-plane modes due to in-plane forces in rotating circular plates [5–7]. However, increasing attention has been given to the in-plane modes in the past few years [8–11]. In-plane dynamics of disks is closely related to the sound radiations. Sound radiation from the in-plane modes of a disk has been assumed to be negligible compared to that from the out-of-plane modes. However, in-plane vibration could generate sufficient sound especially for disks that are relatively thick [9]. For example, the radial components of railway wheel are important in rolling noise [12].

Predictions of the in-plane natural frequencies of circular disks have been treated in a few studies. Holland [1] used trigonometric and Bessel functions to study the free in-plane vibration of circular disks with free edges and presented frequency parameters for different values of Poisson's ratio. Farag and Pan [2] analyzed the modal characteristics of in-plane vibrations of a solid disk with clamped outer edge. These studies were carried

*Corresponding author. Tel.: +1 5145592762; fax: +1 5148483175.
E-mail address: s_bashm@encs.concordia.ca (S. Bashmal).

0022-460X/$ - see front matter © 2008 Elsevier Ltd. All rights reserved.
doi:10.1016/j.jsv.2008.11.024

out for a limited set of boundary conditions. Irie et al. [3] examined the in-plane vibrations in circular and annular disks using transfer matrix formulation. Natural frequencies were obtained for several radius ratios of annular disks with combinations of free and clamped conditions at the inner and outer edges but mode shapes were not presented. Ambati et al. [4] studied in-plane vibrations of solid disks and rings. The natural frequencies and mode shapes were evaluated for general case of annular configuration as hole size increased from thin disks to narrow thin rings. Theoretical results were confirmed by experiments.

Exact solutions in terms of Bessel functions can be obtained for limited cases where the disk is isotropic and subject to classical boundary conditions. Hence, most of the approaches for the solution of vibration problems are approximate in nature. The Rayleigh–Ritz method has been commonly used to study vibration of structures due to its reasonable accuracy and versatility. However, the accuracy of this method depends on the choice of the shape functions that should satisfy at least the geometric boundary conditions. Bhat [13] suggested a set of boundary characteristic orthogonal polynomials for use in the Rayleigh–Ritz method as admissible functions for dynamic and static problems of beams or plates with classical boundary conditions. These functions have some features such as relative ease of generation and integration, diagonal mass matrix and diagonally dominant stiffness matrix. Rajalingham and Bhat used boundary characteristic orthogonal polynomials successfully to study the vibration of a variety of structures such as elliptical plates [14,15].

The classical boundary conditions such as simply supported, clamped or free do not precisely represent the support conditions in practical applications. Using artificial springs at the free boundaries and permitting the spring constants to take specific values any boundary condition can be achieved. Kim and Dickinson [16] studied axisymmetrical and non-axisymmetrical vibrations of isotropic and polar orthotropic annular plates with one or both peripheries elastically restrained against rotation and/or translation using the Rayleigh–Ritz approach.

The main objective of the present paper is to investigate the in-plane vibration of circular disks including annular disks, under combinations of classical boundary conditions. The boundary characteristic orthogonal polynomials [13] are employed as assumed deflection functions in the Rayleigh–Ritz method to obtain the natural frequencies and associated mode shapes. Orthogonal polynomials are generated for the free boundary conditions of the disk and artificial springs are used to account for any possible boundary conditions. The clamped boundary case is also analyzed with orthogonal polynomials that directly satisfy the clamped boundary conditions. The natural frequencies are tabulated and compared with data available in the literature. Mode shapes are presented and discussed.

2. Theory

Let us consider the circular disk shown in Fig. 1. The material of the circular disk is assumed to be isotropic with mass density ρ, Young's modulus E and Poisson's ratio v. The outer radius of the disk is R, the inner radius is R_i and the thickness of the disk is h. The displacement components of a material point on the disk are denoted by u_r, u_θ. The expression for the potential energy of the disk in polar coordinates is derived from the

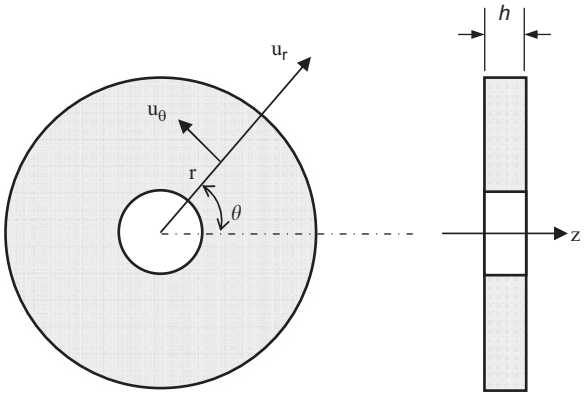

Fig. 1. The natural frequencies of in-plane vibration of a stationary disk.

constitutive laws and strain–displacement relations. The strain energy can be written in polar coordinate system (r,θ) as

$$W = \frac{1}{2}\int_0^R \int_0^{2\pi} (\sigma_r \varepsilon_r + \sigma_\theta \varepsilon_\theta + 2\sigma_{r\theta}\varepsilon_{r\theta}) r \, \mathrm{d}r \, \mathrm{d}\theta. \tag{1}$$

Small strains are assumed and Hooke's law is employed to express stress–strain relationship. For a flat disk, plane stress conditions may be expressed by the following relations:

$$\sigma_r = \frac{E}{1-v^2}(\varepsilon_r + v\varepsilon_\theta),$$

$$\sigma_\theta = \frac{E}{1-v^2}(\varepsilon_\theta + v\varepsilon_r),$$

$$\sigma_{r\theta} = \frac{E}{1+v}\varepsilon_{r\theta}. \tag{2}$$

Substituting Eq. (2) into the strain energy expression (1) leads to

$$W = \frac{1}{2}\int_0^R \int_0^{2\pi} \frac{E}{1-v^2}(\varepsilon_r^2 + 2v\varepsilon_r\varepsilon_\theta + \varepsilon_\theta^2 + 2(1-v)\varepsilon_{r\theta}^2) r \, \mathrm{d}r \, \mathrm{d}\theta. \tag{3}$$

For small deformations, the strain–displacement relations are written as

$$\varepsilon_r = \frac{\partial u_r}{\partial r},$$

$$\varepsilon_\theta = \frac{1}{r}\left(u_r + \frac{\partial u_\theta}{\partial \theta}\right),$$

$$\varepsilon_{r\theta} = \frac{1}{2}\left(\frac{1}{r}\frac{\partial u_r}{\partial \theta} + \frac{\partial u_\theta}{\partial r} - \frac{u_\theta}{r}\right). \tag{4}$$

By substituting strain–displacement relations into Eq. (3), the maximum strain energy is expressed in terms of the displacement as

$$W = \frac{1}{2}\int_0^R \int_0^{2\pi} \frac{E}{1-v^2}\left\{\left(\frac{\partial u_r}{\partial r}\right)^2 + 2v\left(\frac{u_r}{r}\frac{\partial u_r}{\partial r} + \frac{1}{r}\frac{\partial u_\theta}{\partial \theta}\frac{\partial u_r}{\partial r}\right) + \left(\frac{u_r}{r}\right)^2 + 2\frac{u_r}{r^2}\frac{\partial u_\theta}{\partial \theta} + \frac{1}{r^2}\left(\frac{\partial u_\theta}{\partial \theta}\right)^2 + \frac{1}{2}(1-v)\left(\frac{1}{r}\frac{\partial u_r}{\partial \theta} + \frac{\partial u_\theta}{\partial r} - \frac{u_\theta}{r}\right)^2\right\} r \, \mathrm{d}r \, \mathrm{d}\theta. \tag{5}$$

The maximum kinetic energy of the disk can be expressed as

$$T = \frac{1}{2}\int_0^R \int_0^{2\pi} (u_r^2 + u_\theta^2)\omega^2 \rho r \, \mathrm{d}r \, \mathrm{d}\theta. \tag{6}$$

For harmonic vibration with time dependence, the free in-plane vibrational response is assumed to have a sinusoidal variation around the disk, and may be expressed in the form:

$$u_r(r,\theta,t) = \sum_n^\infty U_n(r)\cos(n\theta)\mathrm{e}^{-\mathrm{j}\omega t}, \tag{7}$$

$$u_\theta(r,\theta,t) = \sum_n^\infty V_n(r)\sin(n\theta)\mathrm{e}^{-\mathrm{j}\omega t}. \tag{8}$$

Substituting the assumed solutions, Eqs. (7) and (8), into the energy Eqs. (5) and (6), both equations are integrated with respect to θ from $\theta = 0$ to 2π. The integrals of the trigonometric functions are expressed

by the relations

$$\int_0^{2\pi} \cos(n\theta)\sin(n'\theta)\,\mathrm{d}\theta = 0,$$

$$\int_0^{2\pi} \cos(n\theta)\cos(n'\theta)\,\mathrm{d}\theta = \begin{cases} 0 & \text{for } n \neq n', \\ \pi & \text{for } n = n', \end{cases}$$

$$\int_0^{2\pi} \sin(n\theta)\sin(n'\theta)\,\mathrm{d}\theta = \begin{cases} 0 & \text{for } n \neq n', \\ \pi & \text{for } n = n'. \end{cases}$$

The following equations are obtained:

$$W = \frac{\pi}{2}\frac{E}{1-v^2}\mathrm{e}^{-2\mathrm{j}\omega t}\int_0^R \left\{ (U_n')^2 + 2vU_n'\left(\frac{U_n}{r}+\frac{nV_n}{r}\right) + \left(\frac{U_n}{r}+\frac{nV_n}{r}\right)^2 + \frac{1}{2}(1-v)\left(-\frac{nU_n}{r}+V_n'-\frac{V_n}{r}\right)^2 \right\} r\,\mathrm{d}r\,\mathrm{d}\theta, \tag{9}$$

$$T = \frac{\pi}{2}\rho\omega^2\mathrm{e}^{-2\mathrm{j}\omega t}\int_0^R (U_n^2 + V_n^2) r\,\mathrm{d}r. \tag{10}$$

Introducing the non-dimensional parameter $\xi = r/R$, the displacement $U_n(\xi)$ and $V_n(\xi)$ of circular disks can be expressed as a linear combination of the assumed deflection shapes in form of the boundary characteristic orthogonal polynomial set $\{\phi_1, \phi_1, \ldots, \phi_n\}$ first proposed by Bhat [13]. A starting function $\phi_1(\xi)$ is constructed as the polynomial of the lowest degree that satisfies the geometric boundary conditions. Thus the first polynomial for the present problem is:

$$\begin{aligned} \phi_1(\xi) &= (1-\xi^2)^2 \quad \text{clamped} \\ &= 1 \quad \text{free.} \end{aligned} \tag{11}$$

The successive polynomials are generated using the recurrence relation

$$\phi_2(\xi) = (\xi - b_1)\phi_1(\xi),$$

$$\phi_{k+1}(\xi) = (\xi - b_k)\phi_k(\xi) - c_k\phi_{k-1}(\xi), \quad k \geqslant 2, \tag{12}$$

where

$$b_k = \int_0^1 \xi^2\phi_k^2(\xi)\,\mathrm{d}\xi \Big/ \int_0^1 \xi\phi_k^2(\xi)\,\mathrm{d}\xi, \quad k \geqslant 1,$$

$$c_k = \int_0^1 \xi^2\phi_k(\xi)\phi_{k-1}(\xi)\,\mathrm{d}\xi \Big/ \int_0^1 \xi\phi_{k-1}^2(\xi)\,\mathrm{d}\xi, \quad k \geqslant 2. \tag{13}$$

The displacements are expressed as

$$U_n(\xi) = \sum_m A_{mn}\phi_m(\xi), \tag{14}$$

$$V_n(\xi) = \sum_m B_{mn}\phi_m(\xi). \tag{15}$$

Substituting Eqs. (14) and (15) into Eqs. (9) and (10) and employing the condition $W_{\max} = T_{\max}$, the Rayleigh's quotient can be written as

$$\Omega^2 = \frac{\int_0^1 \left\{ (U_n')^2 + 2vU_n' \left(\frac{U_n}{\xi} + \frac{nV_n}{\xi} \right) + \left(\frac{U_n}{\xi} + \frac{nV_n}{\xi} \right)^2 + \frac{1}{2}(1-v) \left(-\frac{nU_n}{\xi} + V_n' - \frac{V_n}{\xi} \right)^2 \right\} \xi \, \mathrm{d}\xi}{\int_0^1 (U_n^2 + V_n^2) \xi \, \mathrm{d}\xi}, \tag{16}$$

where $\Omega^2 = \rho\omega^2 R^2 (1-v^2)/E$.

Applying the condition of stationarity of Ω^2 with respect to the arbitrary coefficients A_{mn} and B_{mn}, in the form

$$\frac{\partial \Omega^2}{\partial A_{mn}} = 0,$$

$$\frac{\partial \Omega^2}{\partial B_{mn}} = 0, \tag{17}$$

result in the eigenvalue problem

$$([\mathbf{K}] - \Omega^2 [\mathbf{M}]) \begin{Bmatrix} A_{mn} \\ B_{mn} \end{Bmatrix} = \{0\}. \tag{18}$$

The stiffness matrix [**K**] is given by:

$$[\mathbf{K}] = \begin{bmatrix} [\mathbf{UU}] & [\mathbf{UV}] \\ [\mathbf{VU}] & [\mathbf{VV}] \end{bmatrix},$$

and

$$(UU)_{ij} = \int_0^1 \left(\xi \phi_i' \phi_j' + v(\phi_i' \phi_j + \phi_i \phi_j') + \frac{\phi_i \phi_j}{\xi} + \frac{1-v}{2} \frac{n^2}{\xi} \phi_i \phi_j \right) \mathrm{d}\xi,$$

$$(VV)_{ij} = \int_0^1 \left(\frac{n^2}{\xi} \phi_i \phi_j + \frac{1-v}{2} \xi \phi_i' \phi_j' + \frac{v-1}{2} (\phi_i' \phi_j + \phi_i \phi_j') + \frac{1-v}{2} \frac{\phi_i \phi_j}{\xi} \right) \mathrm{d}\xi,$$

$$(UV)_{ij} = \int_0^1 \left(\frac{n}{\xi} \phi_i \phi_j + vn \phi_i' \phi_j + \frac{v-1}{2} n \phi_i \phi_j' + \frac{1-v}{2} n \frac{\phi_i \phi_j}{\xi} \right) \mathrm{d}\xi,$$

$$(VU)_{ij} = \int_0^1 \left(\frac{n}{\xi} \phi_i \phi_j + vn \phi_i \phi_j' + \frac{v-1}{2} n \phi_i' \phi_j + \frac{1-v}{2} n \frac{\phi_i \phi_j}{\xi} \right) \mathrm{d}\xi.$$

The mass matrix [**M**] is given as:

$$[\mathbf{M}] = \begin{bmatrix} m_{ii} & [\mathbf{0}] \\ [\mathbf{0}] & m_{ii} \end{bmatrix},$$

where

$$m_{ii} = \int_0^1 \phi_i \phi_i \xi \, \mathrm{d}\xi.$$

The mass matrix is diagonal because of the orthogonal property of the assumed polynomials. The natural frequencies can be obtained by solving the eigenvalues problem associated with Eq. (18).

The previous formulation can be used to obtain the natural frequencies of annular disks under several combinations of boundary conditions. Let us introduce the parameter $\beta = Ri/R$ which is the ratio between inner and outer radii of the disk. A polynomial of degree four is used to represent the first polynomial in the

Table 1
Coefficients of starting functions satisfying geometrical boundary conditions for annular disk (F = free, C = clamped).

Coefficients	Boundary conditions			
	C–C	C–F	F–C	F–F
a_1	$-\beta^2$	$-\frac{2\beta^2+2\beta^3-3\beta^4+\beta^5}{(\beta-1)^3}$	$-\frac{1-3\beta+\beta^2-3\beta^3+3\beta^4-\beta^5}{(\beta-1)^3}$	1
a_2	$2(\beta+\beta^2)$	$-\frac{2(-2\beta-2\beta^2+2\beta^4-\beta^5)}{(\beta-1)^3}$	$-\frac{2(2\beta+2\beta^2-2\beta^4+\beta^5)}{(\beta-1)^3}$	0
a_3	$-1-4\beta-\beta^2$	$-\frac{2+2\beta+8\beta^2-8\beta^3+\beta^4+\beta^5}{(\beta-1)^3}$	$-\frac{-2-2\beta-8\beta^2+8\beta^3-\beta^4-\beta^5}{(\beta-1)^3}$	0
a_4	$2(1+\beta)$	$-\frac{2(-2\beta+2\beta^3-\beta^4)}{(\beta-1)^3}$	$-\frac{2(2\beta-2\beta^3+\beta^4)}{(\beta-1)^3}$	0
a_5	-1	-1	1	0

orthogonal set (ϕ_1). Then, (ϕ_1) can be written in the general form:

$$\phi_1(\xi)=\sum_{i=0}^{4} a_{i+1}\xi^i. \tag{19}$$

The values for the constants a_{i+1} under different combinations of boundary conditions are listed in Table 1. Note that for the free condition of the inner radius, when $\beta=0$ (solid disk), the polynomial (ϕ_1) will be identical to Eq. (11).

An alternative way to obtain the natural frequencies for the clamped boundary conditions is to use artificial springs with admissible functions that satisfy the free boundary conditions. As the stiffness for artificial springs become very high compared to the disk stiffness, the natural frequencies approach those of clamped conditions. The advantage of using this method can be evident when two or more elastic components need to be connected. Rigid joint between two components can be approximated by increasing the stiffness of artificial springs to approach infinity. Flexible joints can be simulated by assigning the actual values of stiffness for the joint [16]. This is useful especially when comparing with experimental work because it is difficult to experimentally simulate the perfect clamped condition at the boundary.

Artificial springs are distributed in the radial and circumferential direction on both inner and outer edges of the disk. The maximum strain energy stored in the artificial springs is given by

$$\begin{aligned} W_{spring} &= \frac{1}{2}\int_0^{2\pi} K_{ro}[u_r(R,\theta,t)]^2 R\,\mathrm{d}\theta + \frac{1}{2}\int_0^{2\pi} K_{ri}[u_r(R_i,\theta,t)]^2 R_i\,\mathrm{d}\theta \\ &= \frac{1}{2}\int_0^{2\pi} K_{\theta o}[u_\theta(R,\theta,t)]^2 R\,\mathrm{d}\theta + \frac{1}{2}\int_0^{2\pi} K_{\theta i}[u_\theta(R_i,\theta,t)]^2 R_i\,\mathrm{d}\theta \end{aligned} \tag{20}$$

where K represents the stiffness per unit length, subscripts r and θ represent, respectively, radial and circumferential directions and i and o are the inner and outer radii of the disk. The total strain energy is obtained by adding Eq. (20) to Eq. (9). Following the same aforementioned procedure and assuming the polynomial functions that satisfy the free conditions, the eigenvalue problem is solved and the natural frequencies are obtained. This method can be used to have clamped condition at either boundary. For example, to have clamped condition at the inner boundary while the outer boundary remain free, the stiffness in Eq. (20) which refer to inner boundary should have high value while the outer artificial springs have null stiffness.

3. Results

A MATLAB program is developed to obtain the solution of the eigenvalues problem. The frequency parameters computed following the present approach are tabulated for several combinations of boundary conditions. The results are compared with those available in the literature. Table 2 presents the dimensionless frequencies for solid disk with free conditions while Table 3 lists the natural frequencies for clamped disks. The natural frequencies for clamped and free conditions at the inner and outer edges of annular disks are presented in Tables 4–7.

The results obtained by the present method are in full agreement with those of other studies. The frequency parameters are the largest for the clamped–clamped disks, and become smaller in that order for the free–clamped disks, the clamped–free disks and free–free disks. With the increase of the radius ratio, the parameters monotonically increase except for the free-free disks (Table 8).

Table 2
Non-dimensional natural frequencies Ω of in-plane vibration for free conditions with $v = 0.3$.

Mode	$n = 1$		$n = 2$		$n = 3$		$n = 4$	
	Ref. [1]	Present study	Ref. [1]	Present study	Ref. [1]	Present study	Ref. [1]	Present study
1	1.6176	1.6175	1.3877	1.3928	2.1304	2.1303	2.7740	2.7739
2	3.5291	3.5289	2.5112	2.5146	3.4517	3.4515	4.4008	4.4005
3	4.0474	4.0472	4.5208	4.5561	5.3492	5.3490	6.1396	6.1395
4	5.8861	5.8858	5.2029	5.2056	6.3695	6.3691	7.4633	7.4630
5	6.9113	6.9109	6.7549	6.8256	7.6186	7.6182	8.5007	8.5012
6	7.7980	7.7976	8.2639	8.2640	9.3470	9.3465	10.2350	10.2380
7	9.6594	9.6590	8.7342	8.8625	9.8366	9.8361	11.0551	11.0570

Table 3
Non-dimensional natural frequencies Ω of in-plane vibration for clamped conditions with $v = 0.33$.

Mode	$n = 1$		$n = 2$		$n = 3$		$n = 4$	
	Ref. [2]	Present study	Ref. [2]	Present study	Ref. [2]	Present study	Ref. [2]	Present study
1	1.9441	1.9442	3.0185	3.0185	3.9116	3.9117	4.7021	4.7022
2	3.1126	3.1131	4.0127	4.0128	4.9489	4.9490	5.8985	5.8986
3	4.9104	4.9098	5.7398	5.7400	6.5537	6.5538	7.3648	7.3650
4	5.3570	5.3572	6.7079	6.7081	7.9342	7.9345	8.9816	8.9818
5	6.7763	6.7774	7.6442	7.6444	8.5336	8.5338	9.5296	9.5299
6	8.4938	8.4942	9.4356	9.4360	10.2790	10.2795	11.1087	11.1091
7	8.6458	8.6454	9.9894	9.9898	11.3380	11.3385	12.5940	12.5945

Table 4
Non-dimensional natural frequencies Ω of in-plane vibration for free–free annular disk with $v = 0.3$.

Radial ratio (β)	$n = 1$		$n = 2$		$n = 3$		$n = 4$	
	Ref. [3]	Present study	Ref. [3]	Present study	Ref. [3]	Present study	Ref. [3]	Present study
0.2	1.652	1.651	1.110	1.111	2.071	2.072	2.767	2.766
	3.842	3.841	2.403	2.402	3.401	3.400	4.389	4.387
0.4	1.683	1.682	0.721	0.721	1.618	1.619	2.482	2.482
	4.044	4.044	2.451	2.450	3.346	3.345	4.227	4.226

Table 5
Non-dimensional natural frequencies Ω of in-plane vibration for free–clamped annular disk with $v = 0.3$.

Radial ratio (β)	$n = 1$		$n = 2$		$n = 3$		$n = 4$	
	Ref. [3]	Present study	Ref. [3]	Present study	Ref. [3]	Present study	Ref. [3]	Present study
0.2	2.104	2.106	2.553	2.556	3.688	3.693	4.712	4.718
	3.303	3.306	3.948	3.953	4.859	4.808	5.894	5.903
0.4	2.517	2.522	2.721	2.734	3.214	3.219	3.955	3.960
	3.508	3.514	4.147	4.153	4.998	5.005	5.874	5.882

Table 6
Non-dimensional natural frequencies Ω of in-plane vibration for clamped–clamped annular disk with $v = 0.3$.

Radial ratio (β)	$n = 1$		$n = 2$		$n = 3$		$n = 4$	
	Ref. [3]	Present study	Ref. [3]	Present study	Ref. [3]	Present study	Ref. [3]	Present study
0.2	2.783	2.806	3.378	3.394	4.066	4.084	4.802	4.811
	4.060	4.102	4.360	4.382	5.104	5.120	6.003	5.791
0.4	3.429	3.456	4.023	4.046	4.707	4.737	5.287	5.360
	5.306	5.350	5.311	5.348	5.619	5.650	6.289	6.313

Table 7
Non-dimensional natural frequencies Ω of in-plane vibration for clamped–free annular disk with $v = 0.3$.

Radial ratio (β)	$n = 1$		$n = 2$		$n = 3$		$n = 4$	
	Ref. [3]	Present study	Ref. [3]	Present study	Ref. [3]	Present study	Ref. [3]	Present study
0.2	0.919	0.940	1.542	1.561	2.157	2.166	2.778	2.779
	2.121	2.148	2.605	2.616	3.473	3.476	4.408	4.407
0.4	1.281	1.296	1.965	1.982	2.445	2.463	2.911	2.924
	2.691	2.714	2.908	2.924	3.604	3.610	4.492	4.495

Table 8
Non-dimensional natural frequencies Ω of in-plane vibration for clamped conditions with $v = 0.33$ (using artificial springs).

Mode	$n = 1$		$n = 2$		$n = 3$		$n = 4$	
	Ref. [2]	Present study	Ref. [2]	Present study	Ref. [2]	Present study	Ref. [2]	Present study
1	1.9441	1.9442	3.0185	3.0185	3.9116	3.9117	4.7021	4.7021
2	3.1126	3.1131	4.0127	4.0128	4.9489	4.9490	5.8985	5.8986
3	4.9104	4.9098	5.7398	5.7400	6.5537	6.5538	7.3648	7.3650
4	5.3570	5.3571	6.7079	6.7081	7.9342	7.9344	8.9816	8.9818
5	6.7763	6.7774	7.6442	7.6444	8.5336	8.5338	9.5296	9.5299
6	8.4938	8.4942	9.4356	9.4360	10.2790	10.2803	11.1087	11.1174
7	8.6458	8.6454	9.9894	9.9898	11.3380	11.3388	12.5940	12.5988

It is shown in the tables that the frequency parameters increase as m and n increase. It is only in the case of totally free disk where the minimum frequencies are those with two nodal diameters ($n = 2$). The reason for this is that the first frequency parameters in $m = 1$ group is a rigid body mode with zero value. This value was

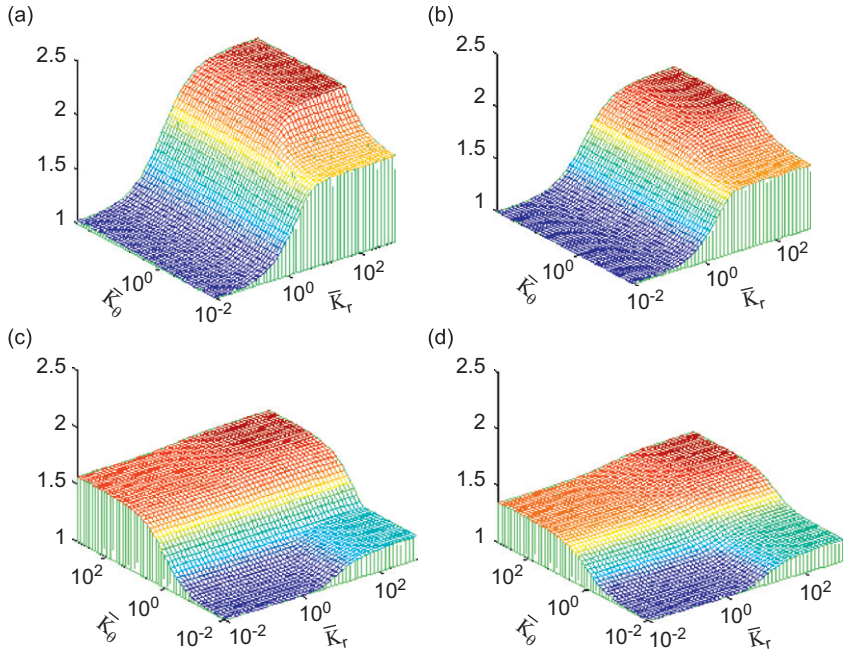

Fig. 2. Effect of artificial stiffness on frequency parameters ($\overline{\Omega}_{m,n} = \Omega_{m,n}/(\Omega_f)_{m,n}$).

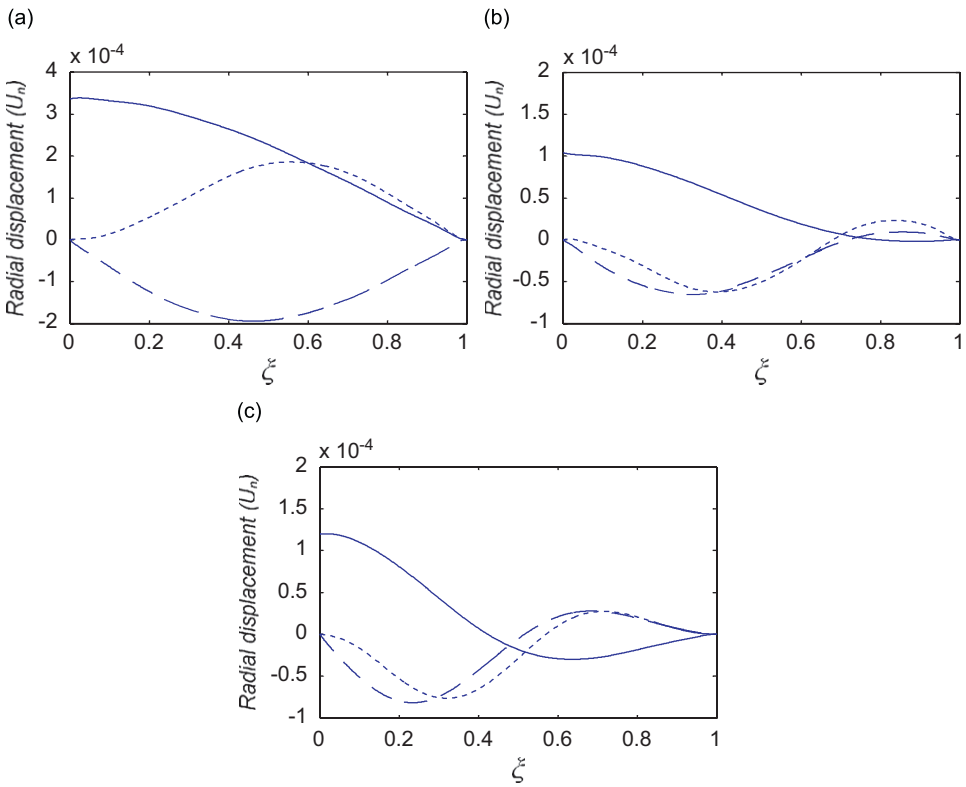

Fig. 3. Radial mode shapes vs. non-dimensional radius: (a) modes with $m = 1$, (b) modes with $m = 2$, and (c) modes with $m = 3$. In each subfigure, — $n = 1$, – – - $n = 2$, …… $n = 3$.

ignored in previous studies. In this study, a value of zero appears in the computations which indicate the existence of rigid mode. If we include this value in Table 2, the fact that frequency parameters increase with m and n is correct even for the free conditions.

It may be useful to use artificial springs to see how frequency parameters develop as spring stiffnesses change from zero (free condition) to infinity (clamped conditions). For a disk clamped at the outer edge and free at the inner edge (Table 3) as the stiffness of the outer edge is reduced, the frequency parameter for mode (1, 1) approaches zero which shows the existence of a rigid body mode. Fig. 2 illustrates the influence of spring stiffness at the outer edge on the frequency parameters of selected modes. In this three-dimensional figure, different combinations of non-dimensional spring stiffnesses, $\overline{K}_r = K_r R(1-v^2)/Eh$ and $\overline{K}_\theta = K_\theta R(1-v^2)/Eh$, are located on the x–y plane and the z-axis is the frequency ratio, $\overline{\Omega}_{m,n} = \Omega_{m,n}/(\Omega_f)_{m,n}$, where $(\Omega_f)_{m,n}$ is the frequency parameter corresponding to the disk with free edge given in Table 2. It is shown that, for lower modes, $\overline{K}_r$ increases the frequency more effectively than $\overline{K}_\theta$. For higher modes the effect of $\overline{K}_\theta$ becomes more significant, although the influence of spring constant becomes insignificant as m and n increase.

Radial distribution of the mode shapes are depicted in Fig. 3 for the first three modes for the case of clamped at the outer edge and free at the inner edge. The center is a nodal point with zero deflection for all modes except for modes with $m = 1$. The component of the response at $\theta+\pi$ is added to the response at θ due to the change of the sine and cosine functions when the angle is increased by π [2].

4. Conclusions

The characteristics of in-plane vibration for circular disk are investigated under different combinations of boundary conditions. The Rayleigh–Ritz method is employed to obtain the natural frequencies of the circular annular disks. The natural frequencies are tabulated and compared with data available in the literature.

The displacements are represented by trigonometric functions in the circumferential direction and by boundary characteristics orthogonal polynomials in the radial direction in the Rayleigh–Ritz method. The results by the present approach compare very well with those available in literature.

References

[1] R. Holland, Numerical studies of elastic-disk contour modes lacking axial symmetry, *Journal of Acoustical Society of America* 40 (1966) 1051–1057.
[2] N.H. Farag, J. Pan, Modal characteristics of in-plane vibration of circular plates clamped at the outer edge, *Journal of the Acoustical Society of America* 113 (2003) 1935–1946.
[3] T. Irie, G. Yamada, Y. Muramoto, Natural frequencies of in-plane vibration of annular plates, *Journal of Sound and Vibration* 97 (1984) 171–175.
[4] G. Ambati, J.F.W. Bell, J.C.K. Sharp, In-plane vibrations of annular rings, *Journal of Sound and Vibration* 47 (1976) 415–432.
[5] S. Yano, T. Kotera, Instability of the vibrations of a rotating thin disk due to an additional support, *Archive of Applied Mechanics* 61 (1991) 110–118.
[6] N.S. Ferguson, R.G. White, The free vibration characteristics of a clamped–free disc under the action of a static in-plane load and constraint on the outer periphery, *Journal of Sound and Vibration* 121 (1988) 497–509.
[7] V. Srinivasan, V. Ramamurti, Stability and vibration of an annular plate with concentrated edge load, *Computers and Structures* 12 (1980) 119–129.
[8] K.I. Tzou, J.A. Wickert, A. Akay, In-plane vibration modes of arbitrarily thick disks, *Journal of Vibration and Acoustics* 120 (1998) 384–391.
[9] H. Lee, R. Singh, Self and mutual radiation from flexural and radial modes of a thick annular disk, *Journal of Sound and Vibration* 286 (2005) 1032–1040.
[10] H. Lee, R. Singh, Comparison of two analytical methods used to calculate sound radiation from radial vibration modes of a thick annular disk, *Journal of Sound and Vibration* 285 (2005) 1210–1216.
[11] N. Baddour, J.W. Zu, Nonlinearly coupled in-plane and transverse vibrations of a spinning disk, *Applied Mathematical Modelling* 31 (2007) 54–77.
[12] D.J. Thompson, C.J. Jones, A review of the modelling of wheel/rail noise generation, *Journal of Sound and Vibration* 231 (2000) 519–536.
[13] R.B. Bhat, Natural frequencies of rectangular plates using characteristic orthogonal polynomials in Rayleigh–Ritz Method, *Journal of Sound and Vibration* 102 (1985) 493–499.

[14] C. Rajalingham, R.B. Bhat, Axisymmetric vibration of circular plates and its analog in elliptical plates using characteristic orthogonal polynomials, *Journal of Sound and Vibration* 161 (1993) 109–118.
[15] C. Rajalingham, R.B. Bhat, Vibration of elliptic plates using characteristic orthogonal polynomials in the Rayleigh–Ritz method, *International Journal of Mechanical Sciences* 33 (1991) 705–716.
[16] C.S. Kim, S.M. Dickinson, The flexural vibration of thin isotropic and polar orthotropic annular and circular plates with elastically restrained peripheries, *Journal of Sound and Vibration* 143 (1990) 171–179.